

NBSIR 82-2517

A Facility to Produce Uniform Space Charge for Evaluating Ion Measuring Instruments

U.S. DEPARTMENT OF COMMERCE
National Bureau of Standards
National Engineering Laboratory
Center for Electronics and Electrical Engineering
Electrosystems Division
Washington, DC 20234

June 1982

Final Report

Prepared for
Department of Energy
Division of Electric Energy Systems
Washington, DC 20585

QC
100
U56
82-2517
1982
c. 2

JUL 22 1982
not all - info

DL/so

250

10 02-7517

1982

NBSIR 82-2517

**A FACILITY TO PRODUCE UNIFORM
SPACE CHARGE FOR EVALUATING ION
MEASURING INSTRUMENTS**

R. H. McKnight and F. R. Kotter

U.S. DEPARTMENT OF COMMERCE
National Bureau of Standards
National Engineering Laboratory
Center for Electronics and Electrical Engineering
Electrosystems Division
Washington, DC 20234

June 1982

Final Report

Prepared for
Department of Energy
Division of Electric Energy Systems
Washington, DC 20585



U.S. DEPARTMENT OF COMMERCE, Malcolm Baldrige, *Secretary*
NATIONAL BUREAU OF STANDARDS, Ernest Ambler, *Director*

TABLE OF CONTENTS

	Page
LIST OF FIGURES	iv
Abstract	1
1. INTRODUCTION	2
2. EXPERIMENTAL APPROACH	3
2.1 Ionization Sources	3
2.2 Dispersal of Ions	4
2.3 Instrumentation	6
2.4 Evaluation of Ion Source Configurations	7
3. DESIGN, CONSTRUCTION, AND TESTING OF A PERMANENT AIR FLOW FACILITY .	12
4. RESULTS	15
5. DISCUSSION	19
5.1 Source Calculations	19
5.2 Ion Loss to Walls	25
6. CONCLUSIONS	29
7. REFERENCES	30

LIST OF FIGURES

		Page
Figure 1.	Schematic (top view) of the prototype standard space charge source	5
Figure 2.	Corona ion source configurations, drawn to scale	8
Figure 3.	Space charge density produced by one wire (source (b), fig. 2) and three wire (source (d), fig. 2) source configurations	9
Figure 4.	Comparison of ion densities produced by two different corona sources with three and seven wires, respectively	10
Figure 5.	Isometric presentation of measurements of the ion density in the test volume determined by using an absolute filter	11
Figure 6.	Attenuation of space charge density by an electrical filter	13
Figure 7.	Top view of permanent low-speed air flow facility to produce space charge	14
Figure 8.	Net space charge measurements made at midplane at locations II, III, and IV (fig. 7)	16
Figure 9.	Net space charge measurements made at midplane at locations II, III, and IV (fig. 7)	17
Figure 10.	Net space charge measurements made at midplane at locations II, III, and IV (fig. 7)	18
Figure 11.	Geometry used in calculations of electrostatic potentials in wire-duct geometry. Two-dimensional modeling is assumed	20
Figure 12.	Equipotential plots for a single wire in a duct	22
Figure 13.	Equipotential plots for the full two-dimensional wire-duct problem	23
Figure 14.	Equipotential plots for wire-duct geometry	24
Figure 15.	Observed decrease in space charge density downstream from ion source (see fig. 1)	27
Figure 16.	Geometry used in theoretical development to explain ion loss in flow facility	28

A FACILITY TO PRODUCE UNIFORM SPACE CHARGE FOR
EVALUATING ION MEASURING INSTRUMENTS

R. H. McKnight and F. R. Kotter

Abstract

A low-speed wind tunnel containing space charge has been constructed and evaluated. The facility is used for testing the performance of ion counters and net space charge measuring devices. Depending on location within the system, space charge densities range from $2 - 7 \times 10^{-8}$ C/m³. The space charge density is spatially uniform within $\pm 5\%$ over more than 90% of the cross sectional area of the test volume, but decreases by approximately 20% between two positions separated by 1 m. Ion densities achieved in this system are comparable to those found near high voltage dc transmission lines but are free from the accompanying large electric fields.

Key words: electrostatic potential; high efficiency air particulate (HEPA) filters; ion counters; ion density; measurement; net space charge.

1. INTRODUCTION

Concern about environmental effects in the vicinity of high voltage direct current (HVDC) transmission lines has led to interest in determining the electrical environment near such lines. Because the parameters of interest are generally the same as those considered by the atmospheric scientist, it is natural to investigate the use of the previously developed instruments in the transmission line context. The development and use of instruments designed to determine electrical parameters associated with atmospheric electricity phenomena has concerned atmospheric scientists for many decades. A variety of devices have been invented to measure quantities such as electric fields, vertical current density at ground level, space charge densities, conductivity and ion mobilities. Using these instruments to make measurements near a HVDC transmission line is not a routine extension of their intended use, since both the electric field intensity and space charge densities are significantly higher than those encountered in fair weather atmospheric measurements. Because of this, it is necessary to evaluate the performance of the various instruments at levels like those encountered near the HVDC transmission line. In previously reported work, consideration has been given to the operation of devices used to measure electric fields [1]¹ and to sensors for determining vertical current density [2]. A parallel plate facility [1] was developed specifically for that work.

The elementary operation of devices designed to measure ion related quantities such as space charge density (ρ) and air conductivity (λ) can be analyzed theoretically [3], but experimental verification of predicted performance for these instruments has proven elusive due to the lack of a "standard" ion source. The conditions existing near the surface of the earth provide a source of space charge which can be used to compare instruments, but these conditions are not at the control of the investigator and are often highly variable. Radioactive sources have been used to provide ions in various studies but have several drawbacks including radiation safety and lack of control over ion production. The purpose of the effort described here was to develop a source of space charge and a means for distributing this space charge uniformly through a volume which would serve as a "test volume" from which air samples containing ions could be drawn by various measuring instruments. For maximum usefulness and versatility, the space charge in the test volume should be uniformly distributed, temporally smooth, have long-term stability (over a few hours), be controllable, and be unperturbed by the measuring instrument. Various studies, such as losses in ducts, flow rate dependence, etc., can be made without knowing the magnitude of the space charge density. However, if instruments are to be calibrated, the space charge density must be known. This requires a measurement of ρ with estimates of uncertainty. Where the ions making up ρ are predominately of one sign, filtration methods can be used to determine ρ [4]. Ideally, the mobility spectrum of the ions should also be known, but measurement of this spectrum is difficult.

¹Numbers in brackets refer to the literature references listed at the end of this report.

The space charge density produced in the test volume should be comparable to or greater than that found under HVDC lines. Measurements by Bracken, et al. [5] show charge densities as large as 1.3×10^{-8} C/m³, which corresponds to a singly charged ion density of 8×10^4 ions/cm³. Some biological experiments require even higher ion densities [6]. A space charge density of 1.6×10^{-7} C/m³ (10^6 ions/cm³), therefore appears to presently represent a practical upper limit of interest.

A number of methods for meeting the criteria discussed above can be considered. A simple monopolar line located above a ground plane and operated above corona threshold will approximate the transmission line environment outside one pole. The parallel plate system mentioned earlier produces a volume containing both space charge and electric fields. While either system might prove useful for a specific investigation, it is important to have a source of space charge in which there are no externally applied electric fields. Only when such a source is available can studies be made without concern for the effects of external fields on instrument operation. While it is true that the transmission line environment has both electric fields and ions, it is desirable to first determine how instruments respond to different levels of space charge density and then extend these results to the combined ion and electric field environment.

This report describes a facility developed to meet the requirements described above. The approach is deliberately tutorial, since many problems were encountered and solved. Much of the initial effort was exploratory and used a developmental system which could be readily modified. The final system described later in the report evolved from these initial experiments.

2. EXPERIMENTAL APPROACH

In the development of a test volume containing space charge, several different technical areas were encountered. These were (1) the source of ionization, (2) the means of dispersing the ions, and (3) instrumentation to characterize the facility. The following discussion is assembled according to these broad subject areas. A general discussion of design philosophy will be presented first, with specific measurements described later in the report.

2.1 Ionization Sources

Ionization may be produced in several ways, but for practical reasons only corona discharges and radioactive sources were considered. Radioactive sources which emit alpha or beta particles ionize air in the immediate vicinity of the source while photon emitters (gamma or hard x-ray) produce a more extended region of ionization. Because there are no electric fields near the sources (unless externally applied), there is no automatic means for transporting charge away from the source. By contrast, high electric fields are required to initiate and sustain corona discharge. If the applied potential is a dc voltage, then charge of one polarity will be transported along field lines

away from the source of the corona, which may be a fine wire or a pointed conductor. If a radioactive source is electrically biased, then charge of one polarity will also be transported from the region of ionization. In either case a space charge of predominantly one polarity will be present some distance from the source. The ions produced by the sources described above will generally be molecular sized and will have mobilities attributed to "small" or "fast" ions. However, particulates in the vicinity of the source may also become charged. Since the space charge of interest for the present work should be composed almost entirely of small ions, such charged particulates present a complicating factor to be avoided if possible.

An interesting and novel approach to generating space charge was considered and rejected because of the requirement that the space charge be made up of small ions. This approach has been used in a study of charge buildup in large oil tankers during washing and consisted of electrifying a spray of water vapor [7]. This technique produces high space charge densities, but not small ions.

For reasons elaborated below, the bulk of the effort reported here used corona sources. Radioactive sources have been used and are being considered for further use in biological studies of the effects of air ions [8]. In biological experiments such sources offer the advantage of not producing ozone and of being audibly quiet. In his definitive work on ion counters, Tammatt [9] used radioactive sources to evaluate various features of counter performance.

2.2 Dispersal of Ions

Because of the desire to avoid having applied electric fields in the test volume, air flow was chosen to carry the ions from the source of ionization and disperse these ions throughout the test volume. In the initial stages of the project, ions were produced by alpha particle sources. Small fans were used to provide an air stream which transported the ions into closed boxes 1-3 m³ in volume. Additional fans were used to mix the air in the boxes. Air samples containing ions were drawn by aspirating devices from the side of the box and the exhaust air from the devices returned to the box. While sizable ion densities were achieved in this way (10⁴-10⁵ ions/cm³), the spatial distribution was uneven and the observed air conductivity was temporally erratic.

A series of measurements indicated that the lack of a smooth air flow across the source of ionization might be responsible for this unsteady behavior, and so a developmental system based on wind tunnel techniques was constructed. This system, which provided much of the design information for the facility described later, was constructed of heavy duty cardboard and is illustrated schematically in figure 1. An air stream entering the low speed air flow facility passes through a series of screens designed to reduce turbulence and then enters a region of ionization. The air stream carries ions downstream to the test volume from which an air sample can be extracted or into which a measuring instrument may be placed.

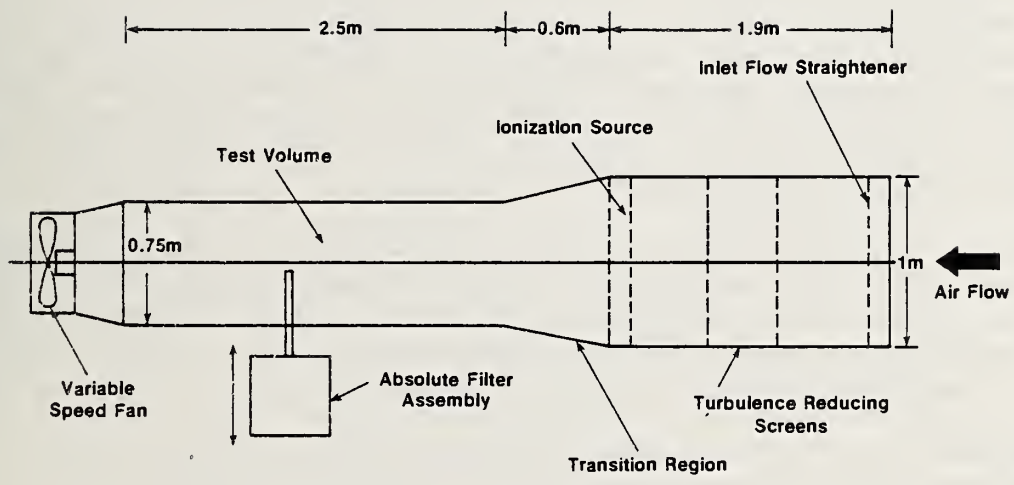


Figure 1. Schematic (top view) of the prototype standard space charge source.

The purpose of this design was (1) to produce a low turbulence air stream at the source, (2) to carry the ions away from the source region in order to avoid stray electric fields, and (3) to provide a sufficiently high volumetric air flow through the facility so that the small volume drawn out by an aspiration device would not significantly perturb the existing space charge density. The admittedly crude mode of construction proved particularly useful, since it was easy to make modifications to the system. Many different source configurations were tried. The cardboard proved sufficiently conductive so that no effects due to surface charging were observed.

2.3 Instrumentation

Air speeds and turbulence in the flow facility were observed using a hot film anemometer. No detailed analysis of the turbulence components was attempted since the space charge density was of primary concern. The hot film anemometer was used near the lower end of the allowable range resulting in estimated errors of as large as $\pm 25\%$ for the air speed measurements. This large uncertainty does not affect the results presented here and would be reduced substantially with improved calibration of the anemometer.

A filtration method employing a high efficiency particulate air (HEPA) or "absolute" filter was chosen to determine the space charge density in the flow system. This technique, which is described in detail elsewhere [4], actually results in a measure of net space charge but for the case of a corona ionization source the space charge is composed almost exclusively of ions of one sign so that the polar space charge and net space charge are nearly equal. In this method, air containing ions is drawn through a HEPA filter which is insulated from ground. Less than 0.1% of the ions pass through the filter [4]. The net space charge density ρ (C/m³) is given by $\rho = I/\phi$, where $I(a)$ is the current due to the ions collected by the filter and ϕ (m³/s) is the volumetric flow rate through the filter.

The filter assembly was configured so that air containing ions was drawn into a sampling tube which extended into the test volume. This entire assembly was moved by means of a leadscrew so that the space charge density was determined at a given point along a horizontal traversal of the test volume. The height of the assembly above the floor of the flow facility could be adjusted as well. In this way, a measure of the spatial distribution of the space charge density in the test volume was determined.

The net space charge density is determined in terms of measured volumetric air flow and ion current. Estimated uncertainty in the current measurement is $\pm 3\%$, while the volumetric air flow uncertainty varies, but may be as large as $\pm 5\%$. An additional source of error involves losses in the sampling tube attached to the filter assembly. All the data presented here were taken at the same flow rate with the same sample tube, so that the relative values are known to $\pm 8\%$. A limited number of measurements were made using different inlet configurations for the sampling tube (elbow, side opening, end opening). There was less than 5% variation in these measurements. In investigating the various inlet configurations, different length sampling tubes were used. Any losses in the tubes themselves were within the uncertainty

of the measurement ($\pm 5\%$). These experiments on sampling losses were not extensive and were made only as part of an assessment of sources of error. More detailed investigations could be made and losses determined for various sampling tube configurations. On the basis of this work, it is conservatively estimated that the space charge densities presented in this report are accurate to $\pm 15\%$. This uncertainty could be reduced substantially by improving volumetric air flow and ion current measurements and making corrections for sampling tube losses.

2.4 Evaluation of Ion Source Configurations

The flow facility illustrated in figure 1 was used to investigate a variety of ionization source configurations, shown in figure 2, all using corona discharges. Since the quantity of interest was the magnitude and spatial variation of the space charge density in the test volume, investigations were made to determine how this quantity depended on source configuration, corona current and air speed at the source. The fan provided three air speeds at the source, 0.56, 0.91 and 1.12 m/s. These air speeds correspond to volumetric flow rates through the facility of approximately 33, 54 and 66 m³/s, respectively. Measurements made near the source using the hot film anemometer indicated the flow to be fairly uniform except near the walls. This was to be expected since the support frames for the turbulence screens protruded into the air stream. The flow straightener shown in the figure was removed early in the work and replaced with a bank of household furnace filters intended to remove large particulates from the air stream.

The source configurations studied are shown in top view in figure 2, where all the corona wires are oriented vertically and are placed between ground "planes" of different geometries. Not shown is a source which consisted of one grounded wire on either side of a corona wire. This source, which was designed to allow the spread of space charge generated in a narrow volume, was abandoned when it was found that corona discharge was initiated on the ground wire at operating voltages of interest. In all sources, the corona wire was 62 μm stainless steel and the discrete wires forming the ground plane were 400 μm bare copper. In source "a" in figure 2, the ground plane was ordinary aluminum window screen. The space between wire and ground plane varied from 0.05 to 0.10 m, with 0.1 m used for most measurements.

Space charge densities were determined at different regions in the test volume by scanning with the absolute filter assembly. Large amounts of data were generated, and only representative results are presented here (figs. 3-5). In general, it was found that the more open sources (b-e) in figure 2 produced greater space charge density, but that the spatial distribution was less uniform and the temporal characteristics less smooth than for the planar source (a). In all cases, the space charge density depended most strongly on the air speed at the source. The yield from the open sources increased somewhat with voltage, but for source (a) the space charge density increased by less than 10% for a change in corona voltage from 6 to 20 kV. The total corona current in this case increased by a factor of more than 10.

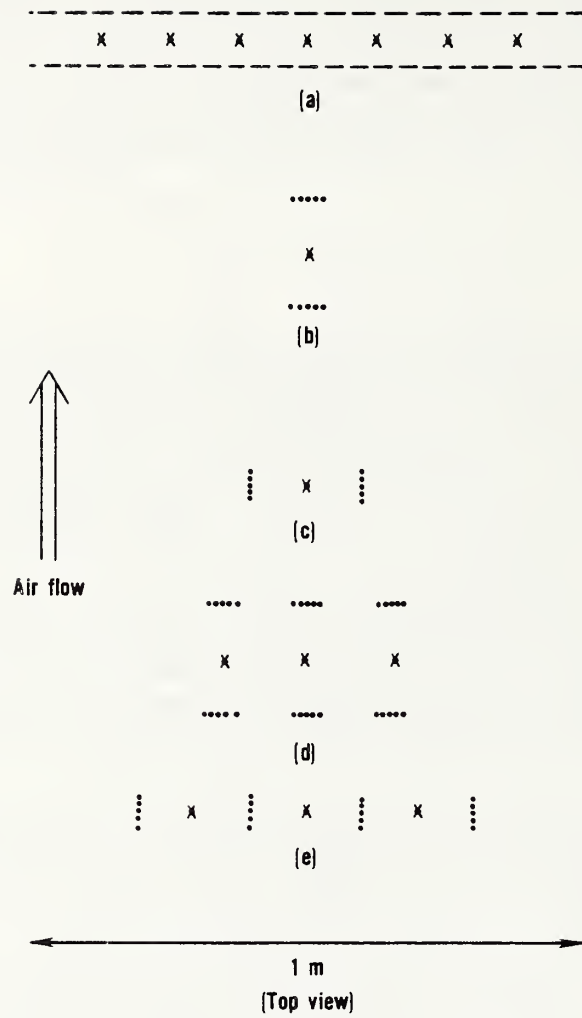


Figure 2. Corona ion source configurations, drawn to scale. Not shown are support frames, insulators, etc., x - corona wires; ---- - grounded screens; - ground wires. The corona wires are 64 μm in diameter.

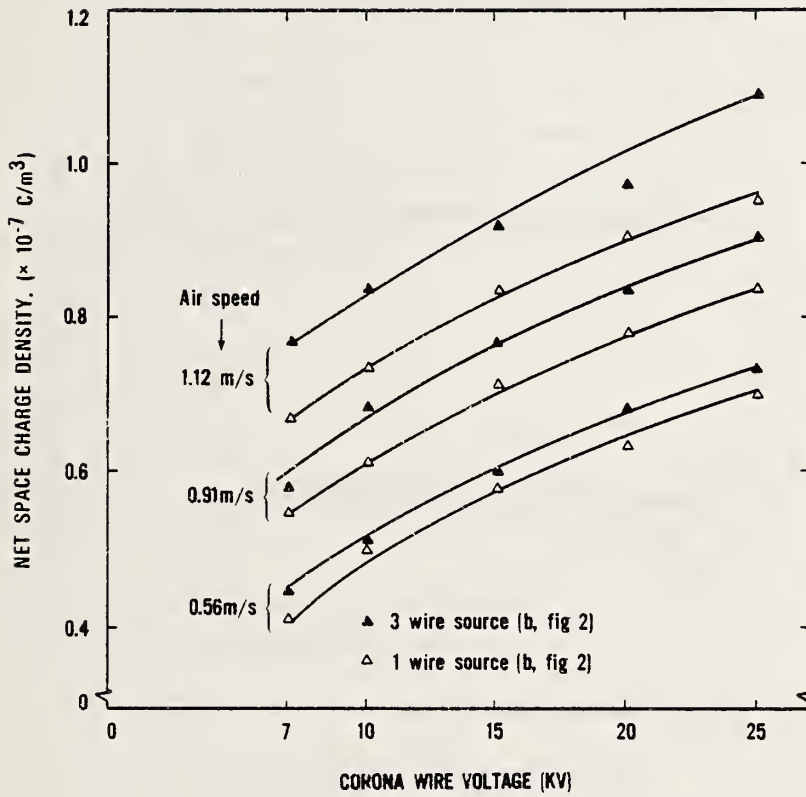


Figure 3. Space charge density produced by one wire (source (b), fig. 2) and three wire (source (d), fig. 2) source configurations. Air speeds shown are at the source. Errors associated with space charge measurements are estimated to be $\pm 15\%$.

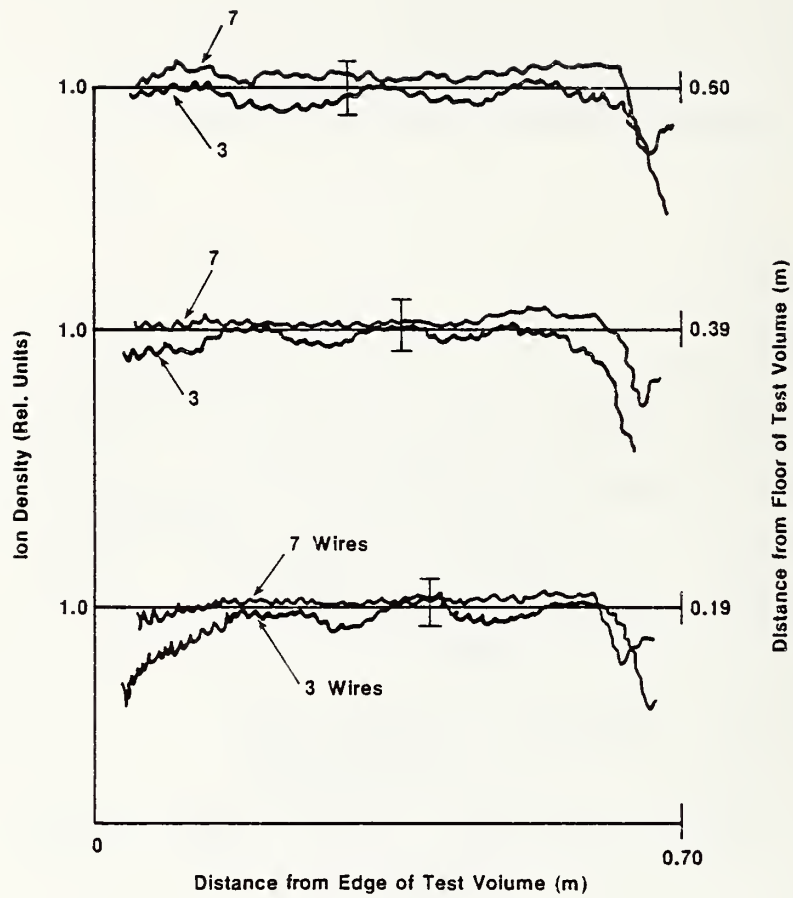


Figure 4. Comparison of ion densities produced by two different corona sources with three and seven wires, respectively. Scans across the test volume were made at selected distances above the floor of the test volume. For each set of measurements the corona voltage was 10 kV and the air speed 1.1 m/s.

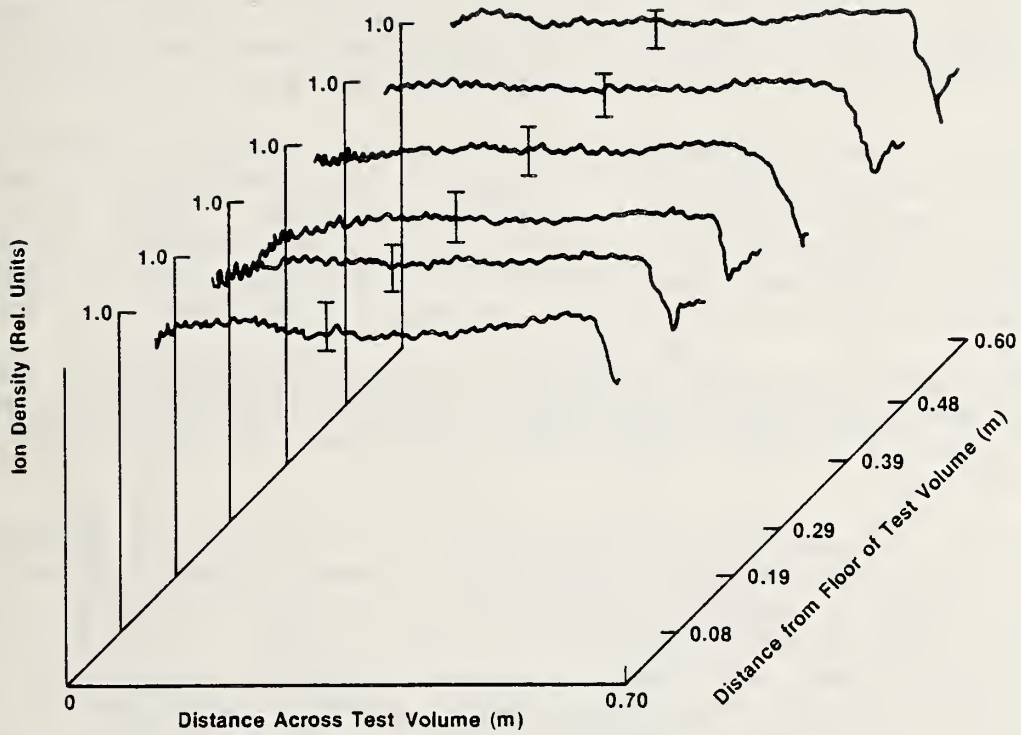


Figure 5. Isometric presentation of measurements of the ion density in the test volume determined by using an absolute filter. Scans were made at different distances above the floor of the test volume as indicated. Corona source voltage was 10 kV and the air speed in the system was 1.1 m/s.

In figure 3, results obtained for sources (b) and (c) in figure 2 are shown. The space charge density displayed is the average measured at midplane in the test volume approximately 2 meters from the source. The planar source (a) in figure 2 produced the most spatially uniform and temporally smooth space charge density, although at a slightly lower level, and so this source configuration was chosen for use in the permanent facility described later.

Figure 4 shows a comparison of ion densities produced by three and seven wire planar sources while figure 5 presents in an isometric plot scans made across the test volume at different distances above the floor. Except for the region near the walls, the uniformity is excellent. The error bars in figures 4 and 5 represent $\pm 5\%$ variation. The falloff on the right hand side is a sampling artifact due to flow perturbation as the sampling tube inlet nears the wall.

Measurements were made at different distances downstream from the source, and the space charge density was found to diminish substantially as the distance from the source increased. This point is discussed in further detail later in section 5.2.

In order to evaluate the performance of an ion measuring instrument (for example, an ion counter) over a wide range of space charge densities, it is necessary that this quantity be variable. As is seen in figure 3, a large variation cannot be obtained by varying corona voltage. If the air flow is to remain constant, some other means of changing ρ must be devised. A simple electrostatic retarding assembly (actually a repelling grid) and the response of ρ in the test volume to changes in the grid voltage are indicated in figure 6. The substantial charge density transmitted for retarding voltages above 300 V indicates a charge component with low mobility. The use of a retarding assembly like this is probably not advisable, since it modifies the mobility spectrum of the ions. This will then influence the response of a measuring instrument that has a mobility dependent response. Control of the ion density remains a problem to be considered in future work.

3. DESIGN, CONSTRUCTION, AND TESTING OF A PERMANENT AIR FLOW FACILITY

Based on the work described above, a permanent air flow system was designed and constructed. The system is shown in figure 7. Air flow characteristics were improved over those for the system illustrated in figure 1 by using a larger area convergence ratio (4:1), eliminating support structures which protrude into the air stream and using a smooth transition section to maintain minimum turbulence of the air stream in the test section. Although not utilized in the work reported here, provision has been made to install a continuously variable speed fan for future work.

The system is also constructed so that HEPA filters can be installed at the inlet to ensure air entering the source region is free of particulates. Except for the transition section, which is lined with 1/8 inch hardboard, the system was constructed using plywood. To investigate possible charging of the walls, measurements were made before and after covering the interior surfaces of the transition section with grounded aluminum foil. No differences were observed and there was no indication of charging of the walls of the system during system evaluation.

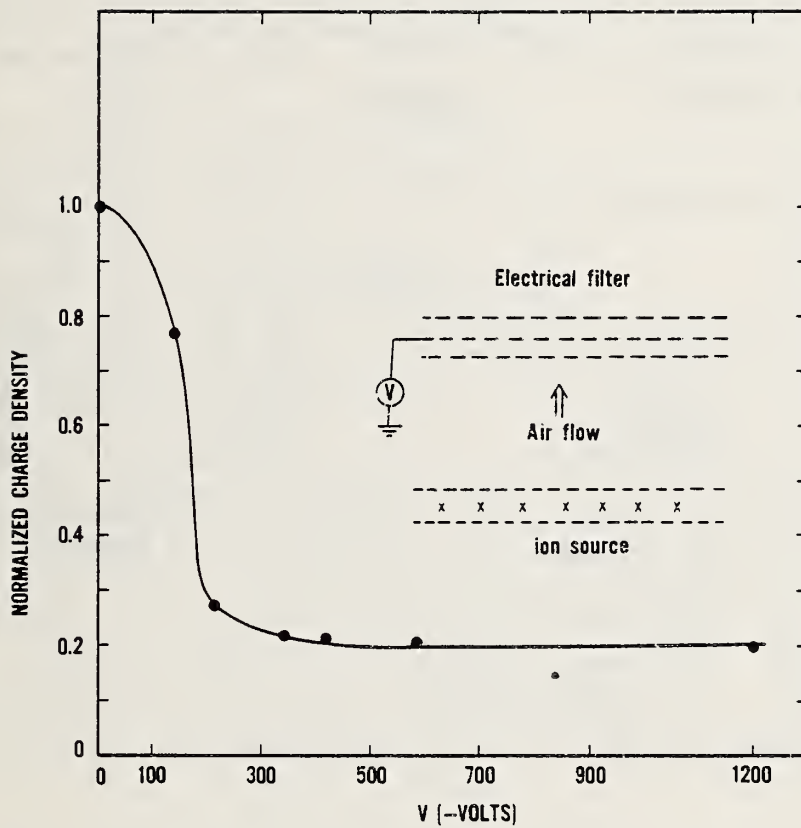


Figure 6. Attenuation of space charge density by an electrical filter. Screen spacing is 0.025 m. The filter-to-source spacing was approximately 0.15 m.

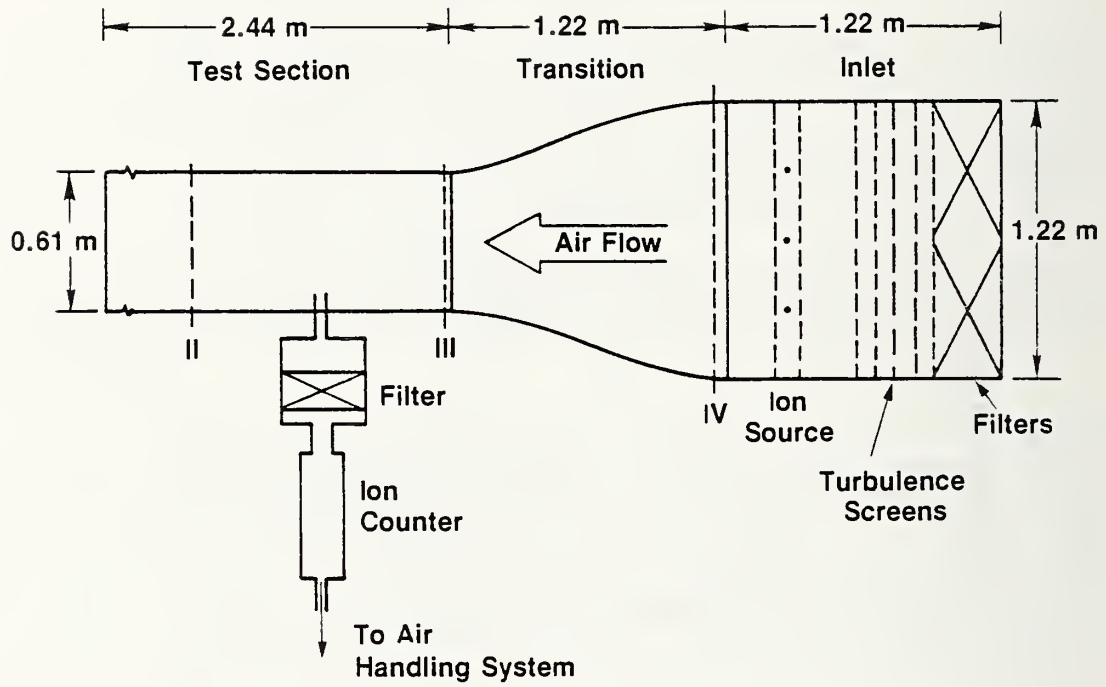


Figure 7. Top view of permanent low-speed air flow facility to produce space charge.

A hot film anemometer was used to characterize the system air flow. Although not ideal, the flow was found to be substantially improved over the earlier system, as was expected. Turbulence levels were significantly lower, and the flow speed was uniform over a larger fraction of the cross section. No attempts were made to improve the flow characteristics, since the space charge produced in the system using an optimized ion source was very uniform. Based on the earlier effort a planar configuration similar to (a) in figure 2 was chosen for the ion source.

4. RESULTS

A series of measurements were made in which different source parameters were varied including:

- (a) Number of corona wires (1, 3, and 9)
- (b) Screen mesh size (5 cm x 5 cm and window screen)
- (c) Corona voltage (7, 10, 15, and 20 kV)
- (d) Air speed at the source (0.5, 0.7, and 0.95 m/s).

For all measurements the screen to corona wire spacing was 10 cm. Not all permutations were examined, although for each source configuration all three air speeds were used. For each source, the absolute filter system was used in a scanning mode to determine the net space charge density at locations II, III, and IV (fig. 7) for five different positions above the floor of the flow system. Representative results of these measurements are displayed on figures 8, 9, and 10. What is shown on these figures is the net space charge density measured at midplane at the three locations of interest. Indicated on the drawings are the relative positions of the inlet and test section walls as well as the locations of the corona wires. All results shown were for a corona voltage +10 kV, air speed at the source of 0.5 m/s and no inlet filters.

In figures 8 and 9, the ground plane was the coarse 5 cm x 5 cm structure and there were one and three corona wires, respectively. The source in figure 10 used nine corona wires and window screen ground planes. This particular configuration was determined earlier to be optimum in terms of the uniformity of space charge density produced in the test section.

There is a substantial decrease in maximum ion density measured near the source (position IV in fig. 7) as the number of corona wires is increased. This result was due to the influence of neighboring corona wires and will be discussed later. The best uniformity was obtained for the nine wire source, a result which is in agreement with the earlier work. The higher ion densities near the walls at position IV are probably due to the influence of the ground support structures on the outer corona wires. A substantial decrease in ion density was noted in going from position IV to position II (fig. 7) as is seen in figures 8-10. Important features of the measurements taken with the new facility are summarized as follows:

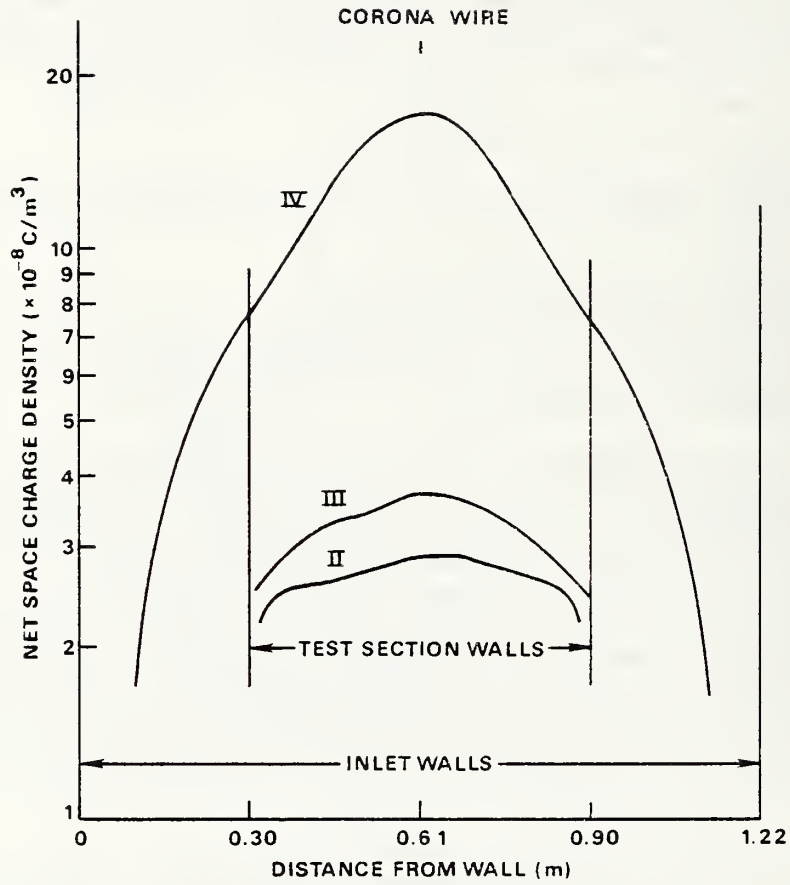


Figure 8. Net space charge measurements made at midplane at locations II, III, and IV (fig. 7). Relative positions of test section inlet walls are shown. Source configuration was one corona wire (position indicated) and coarse ground planes (see text).

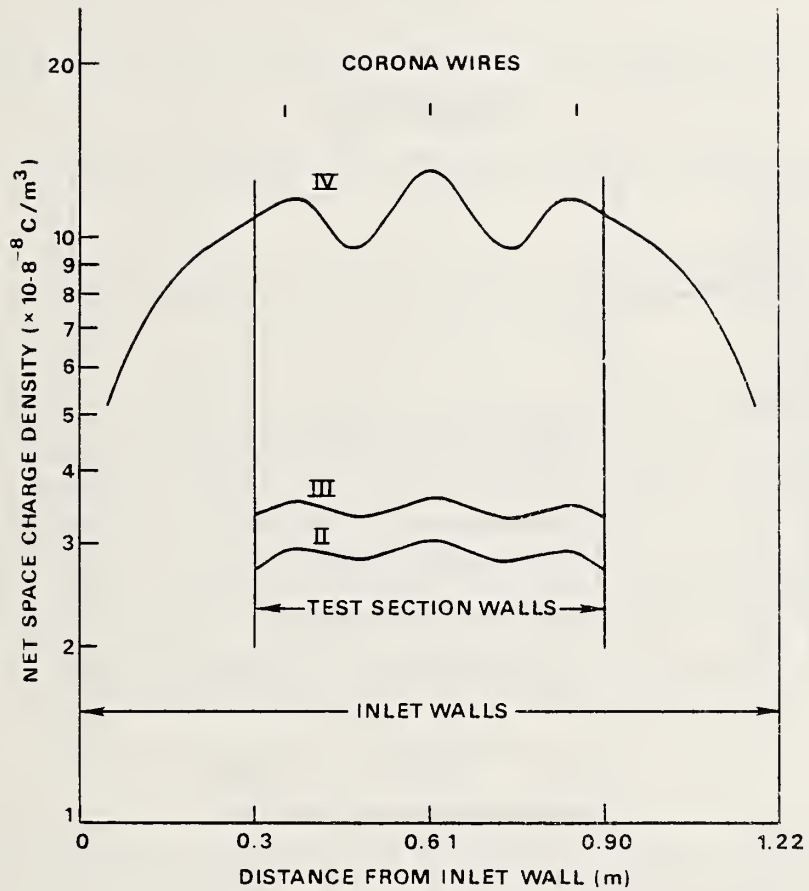


Figure 9. Net space charge measurements made at midplane at locations II, III, and IV (fig. 7). Source configuration was three corona wires (positions indicated) and coarse ground planes (see text).

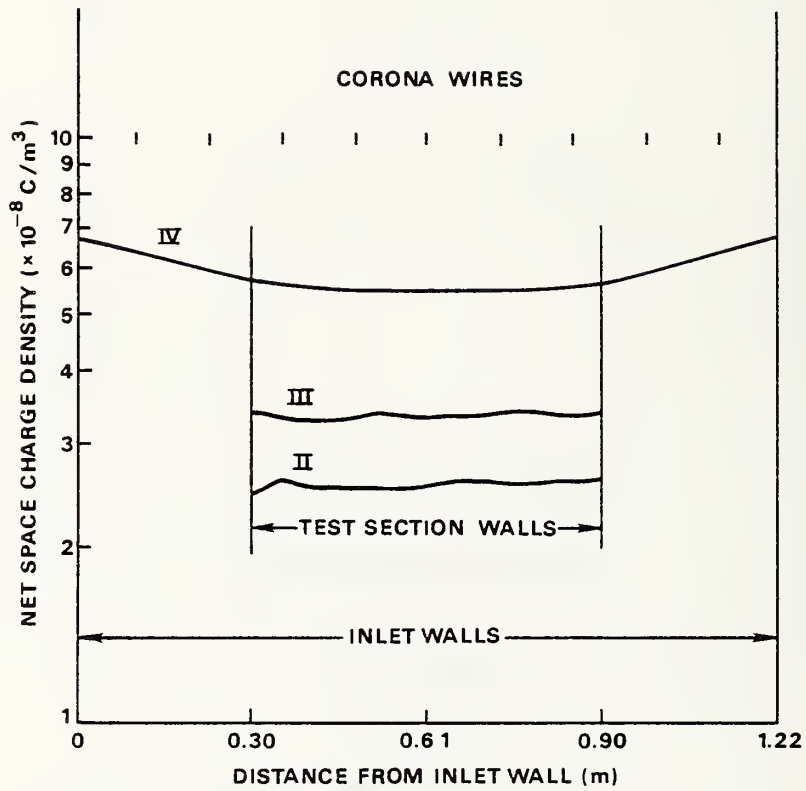


Figure 10. Net space charge measurements made at midplane at locations II, III, and IV (fig. 7). Source configuration was nine corona wires (as indicated) and window screen ground planes.

- (a) The net positive space charge measured in the system ranged from a maximum of $2.5 \times 10^{-8} \text{ C/m}^3$ to $2.2 \times 10^{-7} \text{ C/m}^3$. Assuming singly charged ions, this is a range of ion densities from $1.6 \times 10^5/\text{cm}^3$ to $2.4 \times 10^6/\text{cm}^3$. Negative ion densities were approximately 30% lower. In the test volume itself, the range of space charge density was from $2.5 \times 10^{-8} \text{ C/m}^3$ to $5.7 \times 10^{-8} \text{ C/m}^3$.
- (b) Changes in corona current as large as a factor of 10 result in only a 20% change in measured net space charge.
- (c) The net space charge density decreases by a factor of 2-3 in going from location IV to location II (fig. 7).
- (d) The optimum source configuration for producing a spatially uniform space charge is a multi-wire source with window screen ground planes.

The ion densities actually observed in the test section of the new facility are lower than those measured previously in the developmental system. There are two reasons for this. The distance from source to test section is greater and air speeds at the source are lower in the new system. A system modification to produce substantially higher densities would involve placing an ion source between the test section and the transition. A source in this position could produce as much as a factor of eight greater ion density in the test section. This estimate is based on the effects of higher air speed through the source, which results in a higher ion density (see fig. 3) and a decreased ion loss due to the source being closer to the test volume.

5. DISCUSSION

It is clear from the information in figures 8-10 that the space charge density becomes spatially more uniform and also decreases substantially downstream from the ion source. Also, these figures show that, near the source, a single wire produces a greater maximum space charge density than do sources with three and nine wires. These observations will be discussed in greater detail in this section.

5.1 Source Calculations

The difference in space charge densities produced by different source configurations can be addressed qualitatively by considering the electrical characteristics of the ion source. This region can be modeled using a two-dimensional wire-duct geometry which has been the subject of previous investigations with regard to electrostatic precipitator operation [10,11]. The geometry used is shown in figure 11. A solution of Laplace's equation for the case of one wire in a duct with grounded walls is given below [12].

$$\phi(x,y) = C \sum_{n=1}^{\infty} \frac{1}{n\pi} \left(\sin \frac{n\pi}{2} \right) \left(\sin \frac{n\pi y}{2S_y} \right) e^{-\left| \frac{n\pi x}{2S_y} \right|} \quad (1)$$

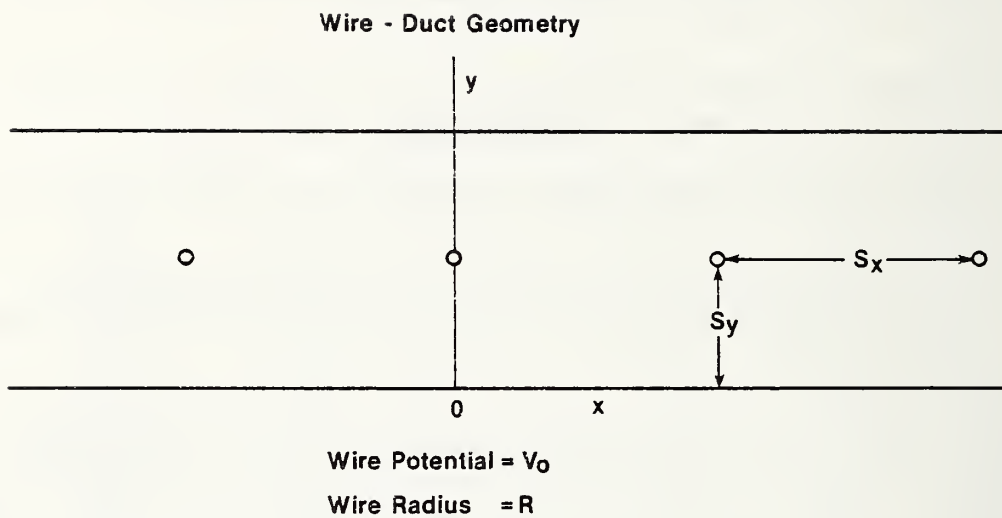


Figure 11. Geometry used in calculations of electrostatic potentials in wire-duct geometry. Two-dimensional modeling is assumed.

$$C = V_0 \frac{\sum_{\substack{n=1 \\ n \text{ odd}}}^{\infty} \frac{1}{n\pi} e^{-\left(\frac{n\pi R}{2S_y}\right)}}{\quad} \quad (2)$$

ϕ is the electric potential, S_y is the wire to plate spacing, R , the wire radius, and V_0 , the wire potential. This solution is applicable for wires located midway between the planes (see fig. 11). The normalization given by eq (2) is obtained by assuming a wire of small dimensions which is not near the walls.

An approximate solution for the situation with an infinite array of wires may be obtained by using the principle of superposition. The general solution is indicated below.

$$\phi = C \left(\sum_{m=0}^{\infty} \sum_{n=1}^{\infty} \frac{1}{n\pi} \sin \frac{n\pi}{2} \sin \frac{n\pi y}{2S_y} e^{-\left|\frac{n\pi}{2S_y} (mS_x - x)\right|} + \sum_{m=1}^{\infty} \sum_{n=1}^{\infty} \frac{1}{n\pi} \sin \frac{n\pi}{2} \sin \frac{n\pi y}{2S_y} e^{-\left|\frac{n\pi}{2S_y} (mS_x + x)\right|} \right) \quad (3)$$

Here the symbols have the same meaning as above and S_x is the wire-to-wire spacing. In practice, the series rapidly converges and for the sources studied here, the contribution from neighboring wires falls off quickly. The formulas here apply only for the case of no space charge. The actual solutions with the wires in corona would involve solving Poisson's equation. This has been done in an approximate way by a number of investigators [14,15]. It was not felt that this complication would substantially improve the understanding of our observations and so only the Laplacian solutions are presented here. In general, as has been shown by MacDonald [14], the presence of space charge distorts the Laplacian solution so the equipotentials shown below would be different for the Poisson's solution. Wind effects have also been neglected.

Calculations were made for the geometries of figures 8-10, where the grounded screens of the source are assumed to be conducting, grounded planes. Plots of the equipotentials are shown in figures 12-14 for the one wire, three wire, and nine wire sources, respectively. Only a limited spatial region is shown. The decrease in fields near a given source wire as additional wires come nearer is evident. This would be expected to affect the current distribution between the ground planes. Such an effect has been reported by Oglesby and Nichols [11]. They show results which indicate that the average current density impinging on the ground plane depends strongly on the wire-to-wire spacing and decreases sharply as the wire-to-wire spacing becomes smaller than below the wire-to-ground plane spacing (fig. 11).

The improved spatial uniformity downstream from the source appears to be due to the effects of the self field of the space charge. Using the maximum space charge measured at location IV (fig. 7) for the one wire source (fig. 8), the field at the surface of an infinitely long cylinder of charge 0.75 m in

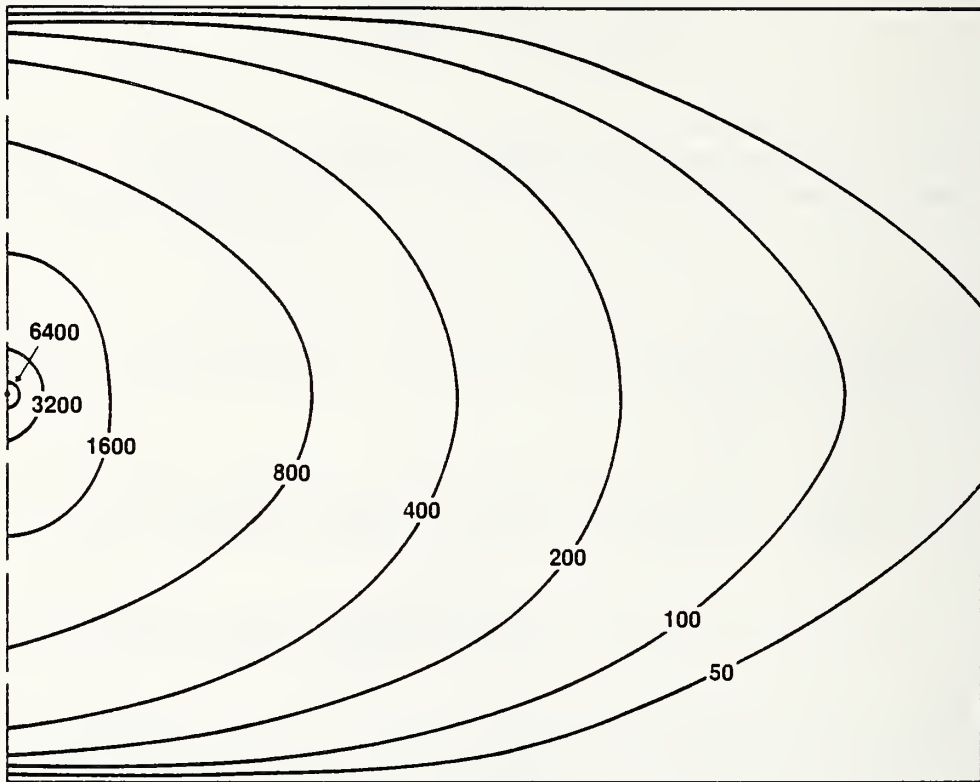


Figure 12. Equipotential plots for a single wire in a duct. Wire-duct spacing was 0.102 m, wire radius 32 μm and wire voltage 10 kV.

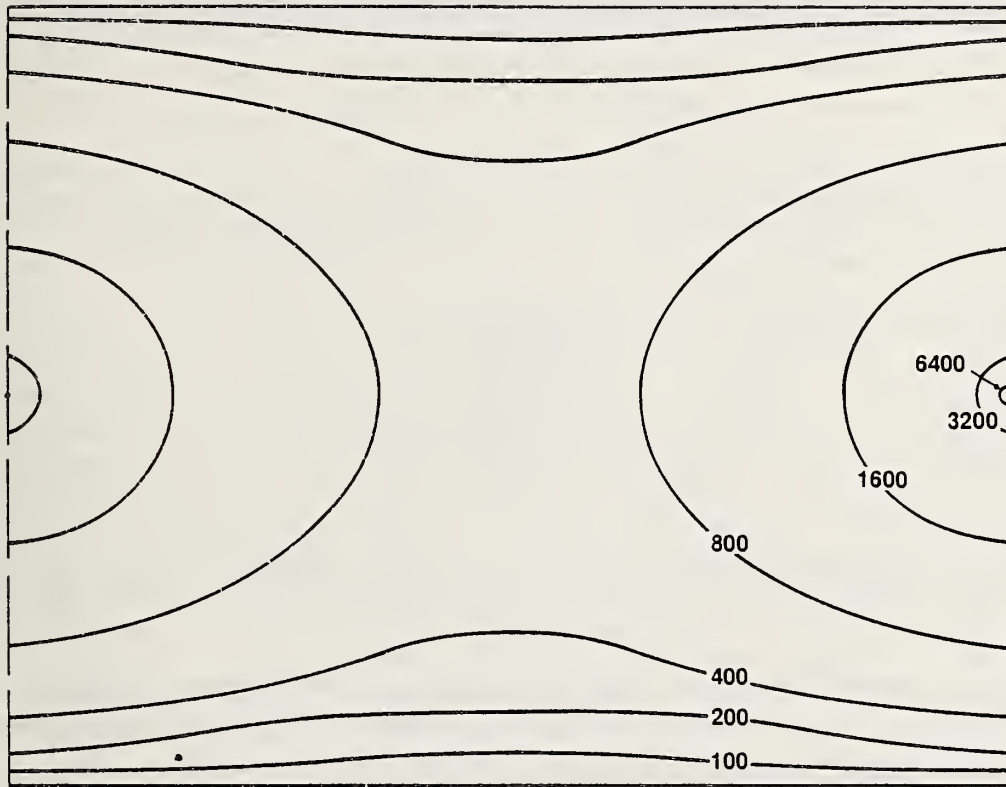


Figure 13. Equipotential plots for the full two-dimensional wire-duct problem. Wire-duct spacing was 0.102 m, wire-wire spacing 0.25 m, wire radius 32 μm and wire voltage 10 kV. This corresponds to the three-wire source.

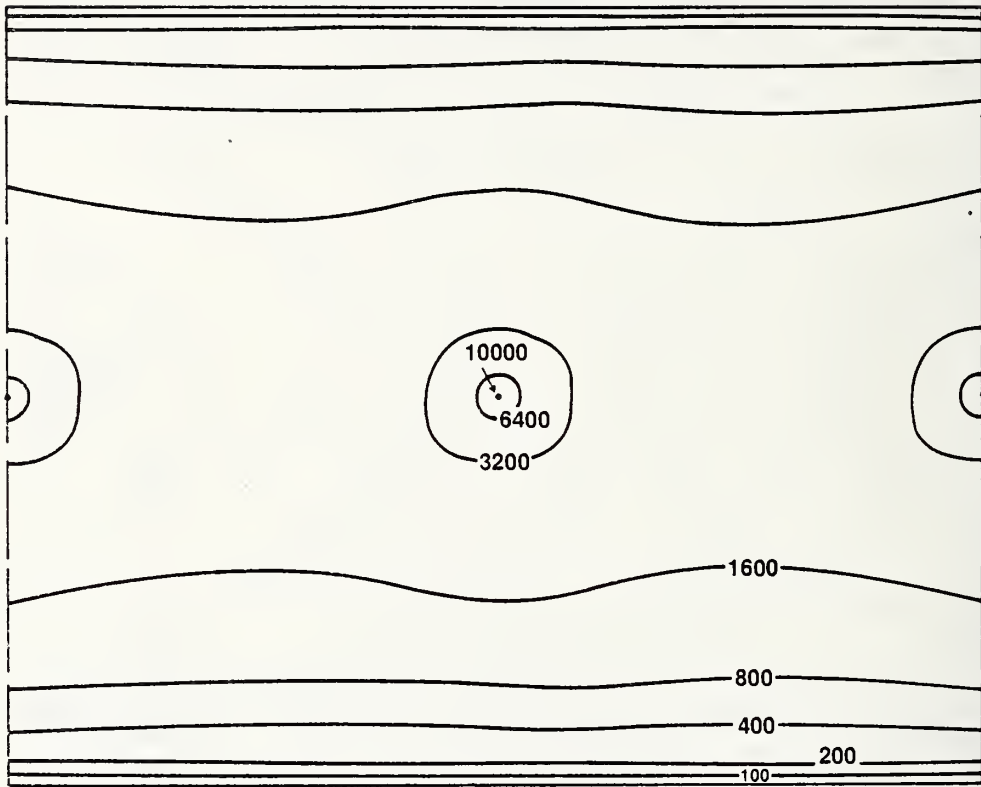


Figure 14. Equipotential plots for wire-duct geometry. Wire-duct spacing was 0.102 m, wire-wire spacing 0.125 m, wire radius 32 μm, and wire voltage 10 kV. This corresponds to the nine-wire source.

diameter is calculated as 3.6 kV/m. The actual fields will differ from this value and will not be uniform, but are substantial enough to cause significant ion motion due to electrical forces for small ions with mobilities of the order of $1 \times 10^{-4} \text{ m}^2/\text{Vs}$. This motion will tend to smooth out a nonuniform distribution.

5.2 Ion Loss to Walls

The decrease in the ion density with increasing distance from the source indicated in figures 8-10 was also observed in the developmental facility. A simple theoretical argument has been developed to provide a qualitative explanation of the observations. Because the theory assumes a constant cross section in the flow facility and the developmental facility more nearly satisfies this criteria, the following discussion is based on results obtained with that system. In figure 15 the ion density as a function of the distance downstream from the ion source (see fig. 1) is indicated. The loss in ion density is due to a number of factors including diffusion, turbulent transport to the walls, and the self field of the space charge itself. Recombination is not a problem, since the space charge is unipolar. Using a simplified diffusion calculation [16], it can be shown that for the transport times through the system involved in the present measurements, an ion would move by diffusion less than 1 cm from its original position (viewed in the rest frame of the ion). Turbulent transport is certainly involved in loss of ions near the walls. The dominant mechanism, however, appears to be that due to the interaction between the ions themselves. A simple model has been developed to consider this problem.

Ions in the system move as a result of wind forces and coulomb interactions between the ions. The electrostatic forces result in an outward drift of the ions with a resultant loss of ions to the wall and a decrease in space charge density downstream from the source as shown in figure 15.

A simple model has been developed in an attempt to verify this explanation for the observed decrease in space charge density. The geometry used in the calculation below is indicated in figure 16. Assume a uniform space charge density ρ_0 enters a cylindrical duct. The air speed in the duct is V_z . At a distance L from the inlet, all of the ions entering the duct outside of a critical radius r_0 will be lost to the wall. The outward motion is caused by the electric field due to the charge entering inside r_0 . In reality, there is a continuous expansion of the ions and a nonuniform space charge density along the axis of the cylinder. The actual ion flow problem is very complicated and not amenable to simple analysis. In the approach taken here, the cylinder of charge inside r_0 is assumed to be long and fixed, so that an expression for the electric field can be derived using Gauss' law. This electric field is given by

$$E(r) = (\rho_0 r_0^2 / 2\epsilon_0)(1/r) \quad r_0 < r < R \quad (4)$$

The equation of motion for the radial movement of an ion can be written as

$$V_r = dr/dt = KE(r) = (K\rho_0 r_0^2 / 2\epsilon_0)(1/r) \quad (5)$$

where K is the mobility of the ion.

Separating variables and integrating

$$\int_{r_0}^R dr = (K\rho_0 r_0^2 \epsilon_0) \int_0^T dt \quad (6)$$

$$(R^2 - r_0^2)/2 = (K\rho_0 r_0^2 / 2\epsilon_0) T \quad (7)$$

Here T is the transit time for the ions from the entrance to $Z = L$, which is equal to L/V_z .

As indicated in figure 15, the laboratory measurements provide a measure of the space charge density downstream from the source. The region near the source is inaccessible. In order to relate the calculation above to the experimental results, it is necessary to derive an expression for the fractional loss in ion density downstream from the source.

It is clear from figure 16 that the ions lost to the wall will enter the duct outside r_0 , while the space charge observed at L will be made up of these ions entering at radii less than r_0 .

Consider the motion of a volume element $\Delta v = \pi R^2 \Delta z$ through the duct. At $z = 0$, the charge in the element is $\rho_0 \Delta v$ while at $z = L$ only the charge initially inside r_0 remains, namely, $\rho_0 \pi r_0^2 \Delta z$. If we assume that this charge has expanded to fill Δv at $z = L$, then the charge density measured at $z = L$ is given by

$$\rho(L) = \frac{Q(L)}{\pi R^2 \Delta z} = \rho_0 \frac{r_0^2}{R^2} \quad (8)$$

Solving eq (7) for r_0^2 and substituting in eq (8),

$$\delta\rho = (\rho_0 - \rho_L) / \rho_0 = (R^2 - r_0^2) / R^2 = K\rho_0 L / (\epsilon_0 V_z + K\rho_0 L). \quad (9)$$

In the development above, it was assumed that all ions had the same mobility. In practice, there is a distribution of ions with different mobilities and so K in eq (9) must be replaced with an average weighted mobility \bar{K} , which is unknown. The remaining calculation involves relating eq (9) to the experimental data which requires knowledge of both \bar{K} and ρ_0 . These were determined by first considering the decrease in ρ between $z = 15$ cm and $z = 68$ cm. By using the space charge density measured at the former location as a starting point, a value of $0.88 \text{ cm}^2/\text{Vs}$ was determined for \bar{K} . In this calculation, an air speed of 0.5 m/s was taken as the average through the tunnel. Then using this value of \bar{K} , ρ_0 at $z = 0$ was determined by using eq (9) and the data point at $z = 15$ cm. This value of ρ_0 was

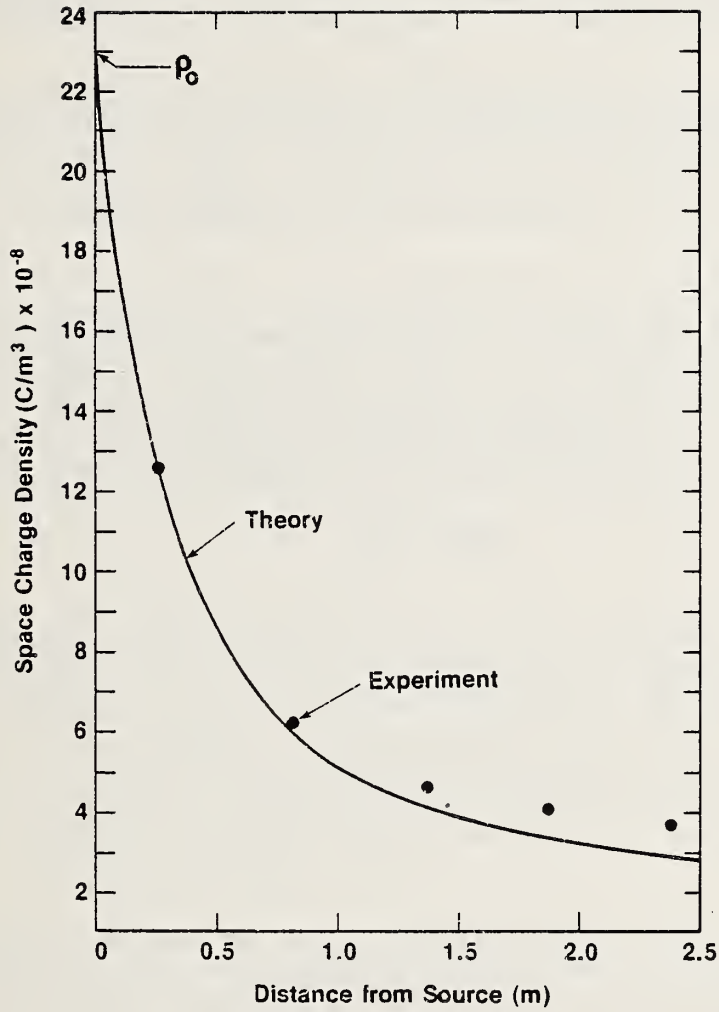


Figure 15. Observed decrease in space charge density downstream from ion source (see fig. 1). Data points - ●. The solid line was calculated using the theory discussed in the text.

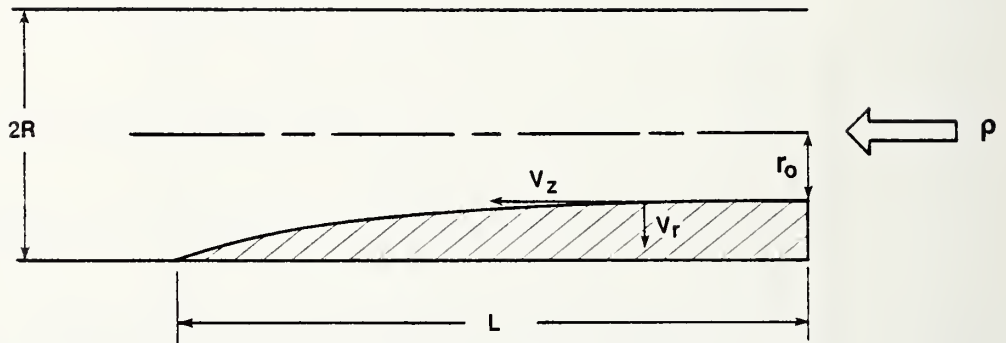


Figure 16. Geometry used in theoretical development to explain ion loss in flow facility. Model is assumed to have cylindrical symmetry.

$2.55 \times 10^{-7} \text{C/m}^3$. This normalization could also have been obtained by using different data points and solving two equations for the two unknowns (ρ_0 and K). Because the air flow in the facility was not constant, there is some uncertainty introduced by using an average speed.

The results of the calculation are shown on figure 15. The excellent agreement between theory and experiment is probably fortuitous, considering the simple theory used. However, these results give considerable support to the proposal that coulomb forces between ions are responsible for the ion losses observed in the low speed air flow facility.

This theoretical prediction agrees remarkably well with the experiment considering the simplicity of the model and the use of an experimental geometry which is square rather than round. It does seem reasonable to conclude that the ion-ion interaction in the space charge itself is the dominant loss mechanism. A similar analysis has not been made for comparable data negative ions. However, the decrease in charge density for negative ions was comparable to that observed for positive ions.

6. CONCLUSIONS

The use of a low-speed air flow facility and a planar corona source has been shown to produce a test volume in which the ion density is uniform to a few percent over the cross sectional area of the test volume. Because of ion losses to the walls, there is a continual decrease in ion density downstream from the source. This decrease is approximately 20% over a 1 m length of the test volume. Near the source space charge densities as high as $2.2 \times 10^{-7} \text{C/m}^3$ were measured. In the test volume itself, the maximum ρ obtained was $5.7 \times 10^{-8} \text{C/m}^3$. These values were determined using a filtration method with an estimated uncertainty of $\pm 15\%$.

The performance of the various ion source configurations studied is qualitatively understood on the basis of electrostatic calculations. Future improvements which would enhance the usefulness of the system include a continuously variable speed fan and a means of controlling the space charge density. It is also desirable that a method be developed to determine the mobility spectrum of the ions present in the system.

The space charge densities measured in the system are significantly larger than those observed under operating HVDC transmission lines. This facility should therefore be useful in evaluating various instruments which measure electrical parameters, which depend on ion density. It has already been used in studying the use of filtration methods for measuring net space charge [4].

The calibration of ion counters or other devices used to determine space charge densities is of importance because of concern about characterizing the electrical environment around high voltage dc transmission lines and in biological exposure systems. One means of doing this is to use a filtration method to determine the space charge density in the air flow facility and compare this density value to that measured by an ion counter. If the ion counter is to be calibrated to within a known degree of uncertainty, then errors in measurement of flow rate, inlet losses, losses in tubes and orientation effects will have to be investigated. The system described in this report is ideally suited for these investigations.

7. REFERENCES

- [1] M. Misakian, Generation and Measurement of DC Electric Fields With Space Charge, *J. Appl. Phys.*, Vol. 52, pp. 3135-3144, 1981.
- [2] R. H. McKnight, F. R. Kotter, and M. Misakian, Measurement of Ion Current Density at Ground Level in the Vicinity of High Voltage DC Transmission Lines, *Nat. Bur. Stand. (U.S.)*, NBSIR-81-2410, 27 pages, 1981.
- [3] J. A. Chalmers, *Atmospheric Electricity*, Pergamon Press, Oxford, England (2nd Ed., 1967).
- [4] R. H. McKnight, The Measurement of Net Space Charge Density Using Air Filtration Methods, *Nat. Bur. Stand. (U.S.)*, NBSIR-82-2486, 28 pages, April 1982.
- [5] T. D. Bracken, A. S. Capon and D. V. Montgomery, Ground Level Electric Fields and Ion Currents on the Celilo-Sylmar \pm 400 KV DC Intertie During Fair Weather, *IEEE Trans. Power Appar. Syst.* PAS 97, p. 370, 1978.
- [6] J. Charry, Rockefeller University (private communication).
- [7] T. E. Owen and R. J. Spiegel, Bulk Carrier Operations Safety Enhancement Project-Phase II, Volume II--Shiptank Electrostatic Model Studies, Final Report for Contract S-38044, U.S. Dept. of Commerce, 1978.
- [8] A. P. Krueger and E. J. Reed, Biological Impact of Small Air Ions, *Science*, Vol. 193, pp. 1209-1213, 1976.
- [9] H. F. Tammet, The Aspiration Method for the Determination of Atmospheric-Ion Spectra, *Scientific Notes of Tartu State University*, Issue 195 (translated from Russian), 1970. Available from the U.S. Dept. of Commerce, Clearinghouse for Federal Scientific and Technical Information, No. TT68-50499.
- [10] H. J. White, *Industrial Electrostatic Precipitation*, Addison-Wesley, Reading, Mass., pp. 95-115, 1963.
- [11] S. Oglesby, Jr. and G. B. Nichols, *Electrostatic Precipitation*, Vol. 8 of *Pollution Engineering and Technology*, Marcel Dekker, pp. 31-55, 1978.
- [12] W.K.H. Panofsky and M. Phillips, *Classical Electricity and Magnetism*, Addison-Wesley, pp. 45-51, 1955.
- [13] P. Cooperman, *Trans. Amer. Inst. Elec. Eng.*, Part 1, pp. 47-50, 1960.
- [14] J. R. McDonald, W. B. Smith, and H. W. Spencer III, A Mathematical Model for Calculating Electrical Conditions in Wire-Duct Electrostatic Precipitation Devices, *Jour. Appl. Phys.* 48, pp. 2231-2243, 1977.

- [15] G. Leutert and B. Böhlen, The Spatial Trend of Electric Field Strength and Space Charge Density in Plate-Type Electrostatic Precipitators, Staub, 32, pp. 27-33, 1972.
- [16] E. W. McDaniel, Collision Phenomena in Ionized Gases, John Wiley & Sons, pp. 488-521, 1964.

U.S. DEPT. OF COMM. BIBLIOGRAPHIC DATA SHEET <i>(See instructions)</i>	1. PUBLICATION OR REPORT NO. NBSIR 82-2517	2. Performing Organ. Report No.	3. Publication Date June 1982
4. TITLE AND SUBTITLE <p style="text-align: center;">A FACILITY TO PRODUCE UNIFORM SPACE CHARGE FOR EVALUATING ION MEASURING INSTRUMENTS</p>			
5. AUTHOR(S) R. H. McKnight and F. R. Kotter			
6. PERFORMING ORGANIZATION <i>(If joint or other than NBS, see instructions)</i> NATIONAL BUREAU OF STANDARDS DEPARTMENT OF COMMERCE WASHINGTON, D.C. 20234			7. Contract/Grant No. 8. Type of Report & Period Covered <p style="text-align: center;">Final</p>
9. SPONSORING ORGANIZATION NAME AND COMPLETE ADDRESS <i>(Street, City, State, ZIP)</i> <p style="text-align: center;">Department of Energy Division of Electric Energy Systems Washington, D. C. 20585</p>			
10. SUPPLEMENTARY NOTES <input type="checkbox"/> Document describes a computer program; SF-185, FIPS Software Summary, is attached.			
11. ABSTRACT <i>(A 200-word or less factual summary of most significant information. If document includes a significant bibliography or literature survey, mention it here).</i> <p style="text-align: center;">A low-speed wind tunnel containing space charge has been constructed and evaluated. The facility is used for testing the performance of ion counters and net space charge measuring devices. Depending on location within the system, space charge densities range from $2 - 7 \times 10^{-8} \text{ C/m}^3$. The space charge density is spatially uniform within $\pm 5\%$ over more than 90% of the cross sectional area of the test volume, but decreases by approximately 20% between two positions separated by 1 m. Ion densities achieved in this system are comparable to those found near high voltage dc transmission lines but are free from the accompanying large electric fields.</p>			
12. KEY WORDS <i>(Six to twelve entries; alphabetical order; capitalize only proper names; and separate key words by semicolons)</i> electrostatic potential; high efficiency air particulate (HEPA) filters; ion counters; ion density; measurement; net space charge.			
13. AVAILABILITY <input checked="" type="checkbox"/> Unlimited <input type="checkbox"/> For Official Distribution. Do Not Release to NTIS <input type="checkbox"/> Order From Superintendent of Documents, U.S. Government Printing Office, Washington, D.C. 20402. <input checked="" type="checkbox"/> Order From National Technical Information Service (NTIS), Springfield, VA. 22161			14. NO. OF PRINTED PAGES 15. Price

